# Molecular Structure of $\mu$-Carbonyl-$\mu$-(dimethylgermylene)-bis(tetracarbonylmanganese)($Mn$–$Mn$)

**Kelly Triplett and M. David Curtis***

*Contribution from the Department of Chemistry, The University of Michigan, Ann Arbor, Michigan 48104.* *Received February 26, 1975*

**Abstract:** The compound, $\mu$-carbonyl-$\mu$-(dimethylgermylene)-bis(tetracarbonylmanganese)($Mn$–$Mn$), forms monoclinic crystals with $a$ = 8.742 (2) Å, $b$ = 14.215 (4) Å, $c$ = 27.221 (7) Å, $\beta$ = 95.05 (2)°, $V$ = 3369.5 Å$^3$, and $Z$ = 8. Systematic absences were consistent with space groups $C_{2/c}(C_{2h}^6)$ or $C_c(C_s^4)$. The structure was successfully refined in the $C_{2/c}$ space group by means of a series of block diagonal refinements to $R$ = 0.062 and $R_w$ = 0.051 based on 2371 ($I > 2\sigma(I)$) counter-collected data with Mo K$\alpha$ radiation. The molecule contains a planar, four-membered ring formed by the two manganese atoms, the bridging germanium, and the carbon of the bridging carbonyl. The ring is distorted with Ge–Mn distances of 2.477 (2) and 2.432 (2) Å, and Mn–C(bridge) distances of 2.037 (8) and 2.154 (7) Å. The distortion is such that longer bonds are on opposite sides of the rhombus. The environment around each manganese is approximately octahedral, with the two octahedra sharing an edge defined by the germanium and bridging carbonyl. The Mn–Mn bond length is 2.854 (2) Å, shorter than that in the nonbridged $Mn_2(CO)_{10}$. This shortening is discussed in terms of the bonding contribution of the bridging atoms. The Mn–Ge–Mn and Mn–C(bridge)–Mn angles are 71.1 (0) and 85.8 (3)°, respectively.

It has been shown that photolysis of bis(metal carbonyl) germanes is a convenient route to complexes containing bridging dialkylgermylene and bridging carbonyl groups (eq 1).[1] These complexes usually exhibit a strong ir band

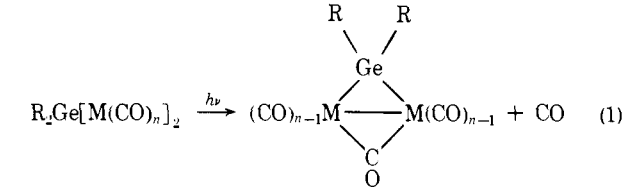

$$R_2Ge[M(CO)_n]_2 \xrightarrow{h\nu} (CO)_{n-1}M(\mu\text{-}GeR_2)(\mu\text{-}CO)M(CO)_{n-1} + CO \quad (1)$$

I, M = Mn; $n$ = 5

ascribable to the bridging CO in the region 1800–1850 cm$^{-1}$. However, the manganese compound, $Me_2GeMn_2(CO)_9$, formed from the photolysis of $Me_2Ge[Mn(CO)_5]_2$, showed only a very weak peak in the bridging region at 1835 cm$^{-1}$ in cyclohexane solution. It was suggested that in solution the manganese complex exists as a mixture of rapidly interconverting isomers with a low concentration of the carbonyl-bridged form, I. Another possi-

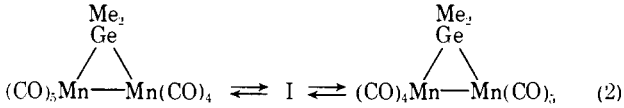

$$(CO)_5Mn(\mu\text{-}GeMe_2)Mn(CO)_4 \rightleftharpoons I \rightleftharpoons (CO)_4Mn(\mu\text{-}GeMe_2)Mn(CO)_5 \quad (2)$$

bility which involved terminal dimethylgermylene groups was also considered.[2] Compounds with terminal group IV, "carbenoid" ligands are known,[3] but those involving germanium have a base filling the remaining coordination site on germanium.[4]

The structure determination reported here was undertaken to provide further insight into the nature of bonding in compound I.

## Experimental Section

Compound 1, prepared as described previously,[1] was crystallized from petroleum ether (30–60°) to give red-orange crystals. An approximately cubic chunk of dimensions 0.17 × 0.20 × 0.20 mm was cut from a larger slab and sealed under nitrogen in a thin walled capillary.

Precession photographs using Mo K$\alpha$ radiation ($\lambda$ 0.7107 Å) indicated a monoclinic crystal with systematic absences $0k0$ ($k = 2n + 1$), $hkl$ ($h + k = 2n + 1$), and $h0l$ ($h = 2n + 1$), consistent with space groups $C_{2/c}(C_{2h}^6$, no. 15) or $C_c(C_s^4$, no. 9). The form was chosen from a consideration of the number of molecules per unit cell (eight), and the numbers of general positions, eight and four, respectively, for the above two space groups. This choice was confirmed by statistical tests during the calculation of normalized structure factors, which indicated a centric crystal, and by the successful refinement. The lattice constants, determined by a least-squares fit to 13 high angle ($25.93 \leq 2\theta \leq 44.94$) reflections, are $a$ = 8.742 (2) Å, $b$ = 14.215 (4) Å, $c$ = 27.221 (7) Å, $\beta$ = 95.05 (2)°, and $V$ = 3369.5 (16) Å$^3$. The density measured by flotation was 1.80 vs. 1.83 g/cm$^3$ calculated.

The crystal was mounted on a Syntex P$\bar{1}$ automated, four-circle diffractometer equipped with a graphite crystal monochromator and scintillation detector using Mo K$\alpha$ radiation ($\lambda$ 0.7107 Å). The $\theta$–$2\theta$ scan technique was used with a scan rate variable from 2° to 24° per min according to peak intensity. The counting rate was corrected for coincidence loss according to:

$$A = [1 - (1 - 4\tau I_o)^{1/2}]/2\tau$$

where $A$ = corrected count rate, $I_o$ = observed count rate, and $\tau$ = dead time of the detector. The integrated intensities and their standard deviations were then computed as follows:

$$I = D(A - B/C)$$
$$\sigma(I) = D(A + B/C^2)^{1/2}$$

where $D$ = scan rate, $B$ = sum of left and right backgrounds, and $C$ = background to scan ratio.

A total of 4359 reflections in the quadrant $hk\bar{l}$ to $hkl$ with $0 \leq 2\theta \leq 55°$ were measured, of which 2371 were classified as observed ($I > 2\sigma(I)$). No absorption correction was applied since the extrema in transmitted intensities were 0.541 ± 5% ($\mu$ = 33.24 cm$^{-1}$).

The program package, XRAY72,[5] was used with the exception that our least-squares refinements used CLS, a locally written program.[6] Atomic scattering factors were taken from Cromer and Weber[7] for all atoms except hydrogen which were taken from the International Tables.[8] The final structure was drawn by ORTEP II.[9]

After applying 1/(LP) corrections, an origin-removed Patterson was interpreted to locate the germanium and two manganese atoms. Full-matrix least-squares refinement of heavy atom positions and isotropic thermal parameters reduced $R$ from 0.42 to 0.31.[10] The function minimized during refinement was $\Sigma w(\Delta F)^2$, where $w = 1/\sigma^2(F)$. $\sigma(F)$ was calculated from the relations:

$$\sigma(I') = (I)/(\mathrm{LP})$$
$$I' = I/(\mathrm{LP})$$
$$\sigma(F) = (I' + \sigma(I'))^{1/2} - (I')^{1/2}$$

A Fourier synthesis then located all non-hydrogen atoms. A series of block diagonal refinements, in which anisotropic temperature factors for all non-hydrogen atoms and anomalous dispersion for

Table I. Final Positional Parameters[a]

| Atom | x | y | z |
|---|---|---|---|
| Mn(1) | 9091 (1) | 4183 (1) | 1066 (1) |
| Mn(2) | 6028 (1) | 3500 (1) | 0869 (1) |
| Ge(1) | 7234 (1) | 4043 (1) | 1677 (0) |
| C(1) | 7749 (9) | 3674 (5) | 0420 (3) |
| C(2) | 4549 (11) | 3387 (6) | 1281 (3) |
| C(3) | 4907 (9) | 3059 (6) | 0322 (3) |
| C(4) | 6645 (10) | 2276 (6) | 1037 (3) |
| C(5) | 5323 (10) | 4697 (6) | 0713 (3) |
| C(6) | 0569 (10) | 4295 (6) | 0657 (3) |
| C(7) | 0190 (11) | 4636 (6) | 1614 (3) |
| C(8) | 3473 (10) | 0397 (6) | 0918 (3) |
| C(9) | 9798 (10) | 2993 (6) | 1232 (4) |
| C(10) | 1457 (15) | 0172 (8) | 1981 (4) |
| C(11) | 7522 (13) | 3115 (8) | 2213 (4) |
| O(1) | 7985 (7) | 3577 (4) | 0010 (2) |
| O(2) | 3528 (8) | 3313 (6) | 1531 (3) |
| O(3) | 4213 (8) | 2781 (4) | −0025 (2) |
| O(4) | 6953 (8) | 1520 (4) | 1131 (2) |
| O(5) | −0187 (8) | 0415 (4) | 0611 (3) |
| O(6) | 1528 (8) | 4364 (5) | 0390 (3) |
| O(7) | 0950 (10) | 4937 (5) | 1944 (2) |
| O(8) | 3212 (8) | 1177 (4) | 0832 (3) |
| O(9) | 0295 (8) | 2270 (4) | 1336 (3) |
| H(1) | 085 (14) | 003 (7) | 227 (4) |
| H(2) | 238 (15) | 031 (8) | 232 (5) |
| H(3) | 091 (9) | 031 (5) | 191 (3) |
| H(4) | 673 (11) | 306 (6) | 237 (3) |
| H(5) | 802 (10) | 266 (6) | 219 (3) |
| H(6) | 813 (12) | 343 (6) | 238 (4) |

[a] All values are ×10⁴. Standard errors for last significant figures are given in parentheses.

Mn and Ge were included, reduced $R$ and $R_w$ to 0.069 and 0.056, respectively. A difference Fourier indicated the hydrogen atom positions, and, while these did not refine satisfactorily, they were included in the final cycles. The final three cycles with all atoms anisotropic except hydrogen converged at $R = 0.062$ and $R_w = 0.051$. On the last cycle, the largest shift was 0.426 of its standard deviation for a positional parameter and 0.547 for a thermal parameter. The final error in an observation of unit weight was 2.01. The final difference Fourier showed peaks as high as 1.36 e/Å³ in the region surrounding the Ge position; but this represents a misplacement of only 2% of the peak height in previous maps. No other peaks were greater than 0.9 e/Å³ which is less than 10% of the normal carbon peak intensity. The final positional and thermal parameters with their standard deviations are listed in Tables I and II.

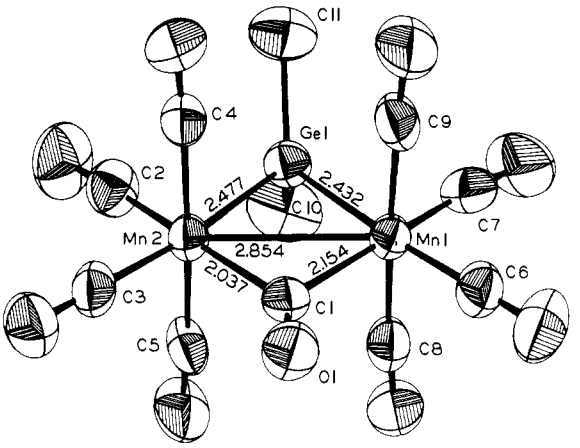


**Figure 1.** ORTEP II drawing of the structure of $(Me_2Ge)Mn_2(CO)_9$. Thermal ellipsoids are drawn at 50% probability.

## Description of the Structure

The molecular structure consists of discrete molecules of $(\mu\text{-}Me_2Ge)(\mu\text{-}CO)[Mn(CO)_4]_2$ with no unusual intermolecular contacts. Figure 1 shows an ORTEP drawing of the molecule and the numbering scheme used. The oxygen atoms of the carbonyls bear the same number as the carbon to which they are bonded. Tables III and IV contain the derived bond distances, bond angles, and a selection of nonbonded distances.

To a first approximation, the coordination about each manganese is octahedral with the two octahedra sharing an edge defined by the germanium atom and C(1) of the bridging carbonyl. The octahedra are distorted due to the spreading of the Ge-Mn-C(1) angles (100.5 (2) and 102.5 (2)°) to accommodate the Mn-Mn bond. There is also a concomitant spreading of the angles between the equatorial (in plane) carbonyls: ∠C(2)-Mn(2)-C(3) = 96.6 (4) and ∠C(6)-Mn(1)-C(7) = 97.0 (4).

To within experimental error, the two manganese atoms, the germanium, and the carbon of the bridging carbonyl are

Table II. Final Anisotropic Thermal Parameters[a,b]

| Atom | $U_{11}$ | $U_{22}$ | $U_{33}$ | $U_{12}$ | $U_{13}$ | $U_{23}$ |
|---|---|---|---|---|---|---|
| Mn(1) | 0371 (7) | 0394 (7) | 0622 (8) | −0017 (6) | 0018 (6) | 0052 (7) |
| Mn(2) | 0349 (7) | 0447 (8) | 0527 (8) | −0017 (6) | 0029 (6) | 0019 (6) |
| Ge(1) | 0535 (6) | 0581 (6) | 0454 (5) | 0003 (6) | 0047 (4) | 0008 (5) |
| C(1) | 0462 (50) | 0387 (46) | 0509 (50) | 0008 (41) | −0013 (41) | 0053 (39) |
| C(2) | 0557 (59) | 0723 (68) | 0738 (66) | 0043 (56) | 0128 (51) | −0012 (54) |
| C(3) | 0372 (49) | 0472 (52) | 0769 (63) | −0016 (43) | 0015 (46) | 0028 (46) |
| C(4) | 0443 (52) | 0636 (57) | 0545 (54) | −0067 (48) | 0011 (43) | 0066 (46) |
| C(5) | 0372 (48) | 0560 (57) | 0780 (65) | 0045 (46) | −0097 (46) | −0091 (50) |
| C(6) | 0486 (56) | 0491 (55) | 0776 (64) | −0083 (46) | 0001 (49) | 0012 (47) |
| C(7) | 0755 (72) | 0577 (59) | 0772 (69) | 0035 (56) | 0071 (58) | 0187 (52) |
| C(8) | 0464 (55) | 0604 (59) | 0741 (66) | −0092 (50) | −0013 (49) | 0001 (50) |
| C(9) | 0376 (52) | 0559 (61) | 1093 (82) | 0027 (47) | −0063 (53) | 0077 (55) |
| C(10) | 1287 (107) | 1124 (93) | 0703 (74) | 0347 (86) | 0255 (74) | −0183 (66) |
| C(11) | 1096 (95) | 0987 (83) | 0705 (71) | 0075 (76) | 0025 (69) | 0190 (62) |
| O(1) | 0625 (40) | 0677 (41) | 0527 (36) | −0070 (35) | 0059 (31) | −0017 (30) |
| O(2) | 0723 (51) | 1538 (74) | 1040 (59) | −0111 (55) | 0363 (44) | −0031 (54) |
| O(3) | 0682 (44) | 0744 (47) | 0775 (45) | −0098 (38) | −0152 (37) | −0044 (37) |
| O(4) | 0802 (48) | 0514 (39) | 0976 (50) | −0044 (38) | 0002 (40) | 0154 (36) |
| O(5) | 0620 (46) | 0581 (42) | 1422 (65) | 0190 (38) | −0099 (44) | 0035 (42) |
| O(6) | 0635 (45) | 0784 (49) | 1132 (57) | −0142 (40) | 0262 (42) | 0001 (41) |
| O(7) | 1271 (72) | 1125 (62) | 0748 (50) | −0228 (56) | −0411 (49) | −0068 (43) |
| O(8) | 0781 (49) | 0454 (37) | 1174 (57) | 0014 (36) | −0019 (43) | 0120 (36) |
| O(9) | 0675 (49) | 0541 (42) | 1796 (76) | 0134 (39) | −0095 (50) | 0231 (47) |

[a] All values are ×10⁴. Standard errors for last significant figures are given in parentheses. [b] The form of the anisotropic thermal ellipsoid is: $\exp(-2\pi^2(U_{11}h^2a^{*2} + U_{22}k^2b^{*2} + U_{33}l^2c^{*2} + 2U_{12}hka^*b^* \cos\gamma^* + 2U_{13}hla^*c^* \cos\beta^* + 2U_{23}klb^*c^* \cos\alpha^*))$.

Table III. Bond Distances and Bond Angles[a]

A. Bond Lengths (Å)

| | | | |
|---|---|---|---|
| Mn(1)–Mn(2) | 2.854 (2) | Mn–C(equatorial) | |
| Mn(1)–Ge | 2.432 (2) | Mn(1)–C(6) | 1.787 (9) |
| Mn(2)–Ge | 2.477 (2) | Mn(1)–C(7) | 1.820 (9) |
| Ge–C(10) | 1.955 (11) | Mn(2)–C(2) | 1.790 (10) |
| Ge–C(11) | 1.967 (10) | Mn(2)–C(3) | 1.822 (8) |
| Mn(1)–C(1) | 2.154 (7) | av. | 1.805 ± 0.023 |
| Mn(2)–C(1) | 2.037 (8) | C–O | |
| Mn–C(axial) | | C(1)–O(1) | 1.159 (9) |
| Mn(1)–C(8) | 1.842 (9) | C(2)–O(2) | 1.175 (12) |
| Mn(1)–C(9) | 1.844 (9) | C(3)–O(3) | 1.146 (10) |
| Mn(2)–C(4) | 1.867 (8) | C(4)–O(4) | 1.132 (10) |
| Mn(2)–C(5) | 1.847 (9) | C(5)–O(5) | 1.137 (11) |
| av. | 1.850 ± 0.012 | C(6)–O(6) | 1.159 (12) |
| | | C(7)–O(7) | 1.151 (11) |
| | | C(8)–O(8) | 1.152 (10) |
| | | C(9)–O(9) | 1.142 (11) |
| | | av. | 1.150 ± 0.013 |

B Bond Angles (deg)

B. Bond Angles (deg)

| | | | |
|---|---|---|---|
| Mn–C–O(axial) | | Mn–C–O(eq) | |
| Mn(2)–C(4)–O(4) | 176.8 (8) | Mn(2)–C(2)–O(2) | 176.8 (8) |
| Mn(2)–C(5)–O(5) | 176.4 (8) | Mn(2)–C(3)–O(3) | 179.4 (17) |
| Mn(1)–C(8)–O(8) | 174.3 (7) | Mn(1)–C(6)–O(6) | 179.8 (29) |
| Mn(1)–C(9)–O(9) | 177.2 (8) | Mn(1)–C(7)–O(7) | 176.2 (9) |
| av. | 176.2 ± 1.3 | av. | 178.0 ± 1.8 |
| Mn–Mn–C(axial) | | Mn–Mn–C(eq) | |
| Mn(1)–Mn(2)–C(4) | 91.4 (3) | Mn(1)–Mn(2)–C(2) | 129.1 (3) |
| Mn(1)–Mn(2)–C(5) | 91.1 (3) | Mn(1)–Mn(2)–C(3) | 134.3 (3) |
| Mn(2)–Mn(1)–C(8) | 91.4 (3) | Mn(2)–Mn(1)–C(6) | 129.1 (3) |
| Mn(2)–Mn(1)–C(9) | 91.3 (3) | Mn(2)–Mn(1)–C(7) | 133.9 (3) |
| av. | 91.3 ± 0.1 | av. | 131.6 ± 2.9 |
| Mn–Mn–O(axial) | | Mn–Mn–O(eq) | |
| Mn(1)–Mn(2)–O(4) | 92.6 (1) | Mn(1)–Mn(2)–O(2) | 130.2 (2) |
| Mn(1)–Mn(2)–O(5) | 92.4 (1) | Mn(1)–Mn(2)–O(3) | 134.1 (1) |
| Mn(2)–Mn(1)–O(8) | 93.6 (1) | Mn(2)–Mn(1)–O(6) | 129.1 (1) |
| Mn(2)–Mn(1)–O(9) | 92.3 (1) | Mn(2)–Mn(1)–O(7) | 135.4 (2) |
| av. | 92.7 ± 0.6 | av. | 132.2 ± 3.0 |
| C–Mn–C | | C–Mn–C | |
| C(2)–Mn(2)–C(4) | 88.4 (4) | C(6)–Mn(1)–C(8) | 89.7 (4) |
| C(2)–Mn(2)–C(5) | 89.0 (4) | C(6)–Mn(1)–C(9) | 89.4 (4) |
| C(2)–Mn(2)–C(3) | 96.6 (4) | C(6)–Mn(1)–C(7) | 97.0 (4) |
| C(3)–Mn(2)–C(4) | 90.1 (4) | C(7)–Mn(1)–C(8) | 88.4 (4) |
| C(3)–Mn(2)–C(5) | 89.1 (4) | C(7)–Mn(1)–C(9) | 89.0 (4) |
| C(4)–Mn(2)–C(5) | 177.2 (4) | C(8)–Mn(1)–C(9) | 177.1 (4) |
| ring atoms | | ring atoms | |
| Mn(1)–Mn(2)–Ge | 53.72 (4) | Mn(2)–Mn(1)–C(1) | 45.4 (2) |
| Mn(2)–Mn(1)–Ge | 55.15 (4) | Mn(1)–Ge–Mn(2) | 71.13 (5) |
| Mn(1)–Mn(2)–C(1) | 48.2 (2) | Mn(1)–C(1)–Mn (2) | 85.8 (3) |

[a] Standard deviations of the last significant figure are given in parentheses. For the averages, the standard deviation was calculated from the formula, $\sigma = [\Sigma (x - \bar{x})^2/n - 1]^{1/2}$.

Table IV. Intramolecular Nonbonded Distances

| Atoms | Distance (Å) | Atoms | Distance (Å) |
|---|---|---|---|
| axial–axial C · · · C | | axial–eq C · · · C | |
| C(4) · · · C(9) | 2.943 (11) | C(2) · · · C(4) | 2.551 (12) |
| C(5) · · · C(8) | 2.934 (12) | C(3) · · · C(4) | 2.611 (11) |
| av | 2.938 ± 0.006 | C(2) · · · C(5) | 2.549 (12) |
| | | C(3) · · · C(5) | 2.573 (11) |
| eq–eq C · · · C | | C(6) · · · C(8) | 2.560 (12) |
| C(2) · · · C(3) | 2.696 (12) | C(7) · · · C(8) | 2.553 (12) |
| C(6) · · · C(7) | 2.701 (13) | C(6) · · · C(9) | 2.553 (12) |
| av | 2.698 ± 0.004 | C(7) · · · C(9) | 2.568 (12) |
| | | av | 2.565 ± 0.020 |
| eq–bridge | | | |
| C(1) · · · C(3) | 2.625 (11) | Mn · · · C (axial) | |
| C(1) · · · C(6) | 2.644 (11) | Mn(1) · · · C(4) | 3.449 (9) |
| av | 2.634 ± 0.13 | Mn(1) · · · C(5) | 3.428 (8) |
| C(2) · · · Ge | 2.664 (8) | Mn(2) · · · C(8) | 3.436 (9) |
| C(7) · · · Ge | 2.738 (10) | Mn(2) · · · C(9) | 3.433 (9) |
| av | 2.701 ± 0.052 | | |

exactly coplanar. The Mn-Mn distance is 2.854 (2) Å, significantly shorter than that observed in $Mn_2(CO)_{10}$ (see below). The symmetry of the molecule is significantly distorted from an idealized $C_{2v}$ symmetry due to the pronounced asymmetry of the Mn(1)-Ge-Mn(2)-C(1) rhombus. The skew is such that the germanium lies closer to Mn(1) while the bridging carbonyl lies closer to Mn(2). Apparently, only one other compound with a Mn-Mn bond bridged by CO is known, namely $[CpMn(CO)(NO)]_2$ in which the CO and NO are disordered in the crystal.[11]

## Discussion

**The Mn–Mn Bond.** The formation of a Mn–Mn bond is required for each Mn atom to assume the 18-electron configuration. The observed Mn-Mn distance, 2.854 Å, is comparable to the Mn-Mn distances observed in other bridged structures, e.g., $(\mu\text{-}SiMe_2)_2[Mn(CO)_4]_2$[12] (2.871 (2) Å)

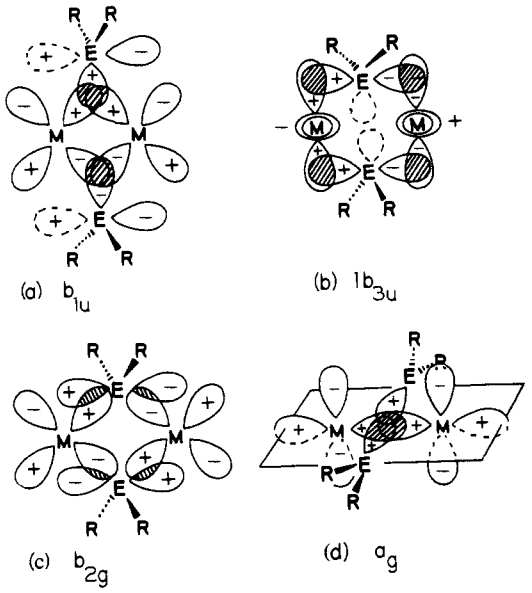


**Figure 2.** Molecular orbitals for the bridge bonds.

and $[CpMn(CO)(NO)]_2$.[11] An apparent exception is $(\mu\text{-H})(\mu\text{-PPh}_2)[Mn(CO)_4]_2$ which has a Mn-Mn distance of 2.937 (5) Å.[13] This apparent anomaly is discussed below. Bridged binuclear complexes with no metal-metal bond normally have much longer Mn-Mn distances, e.g., $[(\mu\text{-Br})Mn(CO)_4]_2$ (3.743 (8) Å),[14] although there are exceptions as has been noted elsewhere.[12]

Further evidence for a Mn-Mn bond is the acute Mn(1)-Ge-Mn(2) angle of 71.13 (5)° which is much smaller than those observed in analogous complexes with no metal-metal bond, e.g., $(\mu\text{-GePh}_2)_2[Fe(CO)_4]_2$[15] (Fe-Ge-Fe = 104.6 (4)°). Other compounds with group 4 bridged metal-metal bonds show similar acute angles; for example, in $[(\mu\text{-SiPh}_2)Mn(CO)_4]_2$,[12] $(\mu\text{-GeMe}_2)(\mu\text{-CO})[CpFe(CO)]_2$,[16] and $[(\mu\text{-GeMe}_2)Ru(CO)_3]_3$,[17] the M-E-M angles are 73.4 (1), 68.15 (3), and 73.4 (1)°, respectively. The acuteness of the angle is determined not only from the lengths of the M-M bond but also from the length of the M-E bond. Thus, for a given M-M bond, larger bridging atoms give more acute angles.

As was also noted in the structure of $[(\mu\text{-SiMe}_2)Mn(CO)_4]_2$,[12] the Mn-Mn bond length in the structure reported here is *shorter* than that in $Mn_2(CO)_{10}$, 2.923 (3) Å.[18] Such shortening of the Mn-Mn bond is unexpected in view of the extreme crowding in these bridged structures and in view of the angle strain associated with the acute Mn-E-Mn (E = Si, Ge) angles. Both effects would tend to lengthen the Mn-Mn bond rather than cause the observed contraction.

A bonding model which rationalizes the observed contraction can be constructed if the bridging $R_2E$ group is considered to be a *bridging* carbenoid ligand (Figure 2).[3,4] Teo et al.[19] have recently performed Fenske-Hall type MO calculations on the bridged manganese species, $[(\mu\text{-PH}_2)_2Mn(CO)_4]_2^{n+}$ ($n$ = 0, 1, 2). The $n$ = +2 species is isoelectronic with $[(\mu\text{-SiMe}_2)Mn(CO)_4]_2$[12] and the compound reported here. Using their MO's as a starting point for a pictorial representation, we expect a strong metal-bridge interaction of the metal and bridge $b_{1u}$ orbital combinations (Figure 2a) and a $\pi$-type interaction of the carbenoid p orbitals and the $1b_{3u}$ metal combination (Figure 2b).

In addition, mixing of the carbenoid p orbital alleviates the anti bonding character of the metal-metal $\pi^*$ ($b_{2g}$) orbital (Figure 2c). These four-center two-electron orbitals offer the conceptual advantage of removing the angle strain implied by picturing the M-E bonds to lie along the lines connecting the nuclei. In the carbenoid model, the regions of electron density are directed toward the center of the rhombus and around its periphery in "bent" bonds of the type in Figure 2b. Thus, by delocalizing the Mn-Mn bonding orbitals, $a_g + b_{1u}$, and by providing some bonding character to the Mn-Mn antibonding orbitals, $b_{2g}$ and $1b_{3u}$, the net Mn-Mn interaction is strengthened and a very short Mn-Mn bond results.

The long Mn-Mn bond, 2.937 (5) Å,[13] of $(\mu\text{-H})(\mu\text{-PPh}_2)[Mn(CO)_4]_2$ might be ascribed to the fact that the hydride 1s orbital cannot provide bonding character to the antibonding interactions, e.g., $b_{2g}$ and $1b_{3u}$; consequently a lower net Mn-Mn bond order obtains. Churchill and Chang[20] have recently discussed the metal-metal bond orders of H-bridged compounds in similar terms.

**The Mn-Ge Bonds.** The germanium of the dimethylgermylene group asymmetrically bridges the Mn-Mn bond. The observed Mn-Ge distances are 2.432 (2) and 2.477 (2) Å. The difference, 0.042 Å, is some 14 times the standard deviation ($\sigma^2(\Delta) = \sigma_1^2 + \sigma_2^2$).

The Mn-Ge distances are shorter than that observed in $Ph_3GeMn(CO)_5$[21] (2.54 Å) and are more similar to the Mn-Ge distance of 2.44 Å observed in $Br_3GeMn(CO)_5$.[22] The Si-Mn distance in $(\mu\text{-SiPh}_2)_2[Mn(CO)_4]_2$ is also shorter than that observed in $Me_3SiMn(CO)_5$, as noted by Simon and Dahl.[12] These authors suggested that the bridging silylene group might be a better $\pi$-acceptor (via Si 3d orbitals) than a terminal $Me_3Si$ group. They also pointed out that the Si 3d orbitals could combine with the $b_{2g}$ metal orbital combinations of Figure 2c. However, later calculations by Teo et al.[19] suggest that the d orbitals (at least on bridging P atoms) play a minor role in the bonding. Similar conclusions on the relatively minor effects of virtual d orbitals have been reached elsewhere.[23] We feel that the four-center molecular orbitals of Figure 2 can account for the observed, short Mn-Ge bonds without invoking enhanced d orbital contributions from the bridging group.

**The Carbonyls.** The metal-carbon distances and angles show interesting variations which appear to arise from a combination of electronic effects and attempts to alleviate nonbonded contacts. The Mn-CO distances trans to the short bridging bonds are significantly shorter than the Mn-CO bonds trans to the long bridge bonds. Thus, the Mn(2)-C(2), trans to the short Mn(2)-C(1) bond, is 1.790 (10) Å, and the Mn(1)-C(6) bond, trans to the short Mn-Ge bond, is 1.787 (9) Å long. These are to be compared with the lengths of the Mn-C bonds, trans to the long Mn-Ge and Mn-C(1) bonds, which are 1.822 (8) and 1.820 (9) Å for Mn(2)-C(3) and Mn(1)-C(7), respectively. On the basis of the $\pi$-bonding model between metal and CO $\pi^*$-orbitals, one might have expected the reverse trend to hold. However, the equatorial carbonyls as a whole do have shorter Mn-C bond lengths than the axial carbonyls, in agreement with the idea that $\pi$-bonding is diminished with a carbonyl trans to a carbonyl. The average axial Mn-C distance is 1.850 ± 0.012 Å or about 0.05 Å longer than the average Mn-C (equatorial) bond.

The presence of the bridging groups, which forces an eclipsed structure on this molecules leads to severe crowding of the carbonyl groups. The average axial-equatorial C···C distance is 2.565 ± 0.20 Å, that for the axial-axial C···C contact is 2.938 ± 0.006, and that for the equatorial-equatorial contact is 2.698 ± 0.004. Kamrass and Lohr[24] have calculated that a collision diameter of 2.75-3.00 Å is appropriate for the van der Waal's interactions between carbonyls in binuclear complexes. It is interesting to note that, even though the axial-equatorial C···C contacts are shorter that the axial-axial C···C contacts, the axial carbon-

yls are inclined *toward* the equatorial carbonyls, i.e., away from the metal-metal bond. The average Mn–Mn–C(axial) angle is 91.3 ± 0.1°. The axial carbonyls are also cocked away from the metal-metal bond with the average Mn–Mn–O(axial) angle being 92.7 ± 0.6°. These data suggest an interaction of the axial carbonyls with the filled $b_{2u}$ (out-of-plane) metal-metal $\pi$-orbital formed from the $d_{xy}$ metal orbitals.[19] This type of interaction has been postulated previously[25] to account for carbonyls bending in *toward* a metal-metal bond, but the possibility of a *repulsive* M–L′ interaction must be considered here.

**Asymmetric Bridges and the Structure in Solution.** The asymmetry of the bridging ligands found in $(\mu\text{-CO})(\mu\text{-GeMe}_2)[\text{Mn(CO)}_4]_2$ places this molecule in "class I" as defined by Cotton and Troup.[26] These authors consider these molecules to be "stop-action" photographs of bridge-opened intermediates which lead to scrambling of bridging and terminal carbonyl groups in compounds, e.g., $Cp_2Fe_2(CO)_4$. This view nicely fits the scheme proposed by Job and Curtis[1] to account for the extremely weak bridging CO bond in the solution spectrum of I. However, the NMR spectrum of I remains unchanged from +80 to −90°, so that bridge terminal exchange is either still rapid at the low temperature, or the compound is in fact nonfluxional. If the latter is the case, then some other mechanism must account for the exceedingly weak ir band of the bridging CO.

We have been unable to obtain really satisfactory solid state ir spectra on compound I. In KBr disks, the compound rapidly decomposes, and in thin films of solid obtained from rapid evaporation of solutions, the bands are extremely broad. The feature at 1835 $cm^{-1}$ is still present, however, and still appears to be anomalously weak. At any rate, we cannot make a definitive assignment of the structure of I in solution on the basis of this solid state structure.

**Acknowledgments.** The authors wish to thank the donors of the Petroleum Research Fund, administered by the American Chemical Society, and the American Metal Climax Foundation, Inc., for support of this research. Special thanks go to Dr. Kenneth Gerst for assistance and advice.

**Supplementary Material Available.** A listing of the observed and calculated structure factors will appear following these pages in the microfilm edition of this volume of this journal. Photocopies of the supplementary material from this paper only or microfiche (105 × 148 mm, 24× reduction, negatives) containing all of the supplementary material for the papers in this issue may be obtained from the Business Office, Books and Journals Division, American Chemical Society, 1155 16th St., N.W., Washington, D.C. 20036. Remit check or money order for $4.50 for photocopy or $2.50 for microfiche, referring to code number JACS-75-5747.

## References and Notes

(1) R. C. Job and M. D. Curtis, *Inorg. Chem.*, **12**, 2514 (1973), and references therein.
(2) M. D. Curtis and R. C. Job, *J. Am. Chem. Soc.*, **94**, 2153 (1972).
(3) J. D. Cotton, P. J. Davison, D. E. Goldberg, M. F. Lappert, and K. M. Thomas, *J. Chem. Soc., Chem. Commun.*, 893 (1974).
(4) T. J. Marks and A. R. Newman, *J. Am. Chem. Soc.*, **95**, 769 (1973).
(5) J. M. Stewart, F. S. Kundell, and J. C. Baldwin, "The XRAY System of Crystallographic Programs", University of Maryland, 1972.
(6) J. W. Schilling, "Fortran IV Crystallographic Least Squares Program", The University of Michigan, 1965.
(7) D. T. Cromer and J. T. Weber, *Acta Crystallogr.*, **18**, 104 (1965).
(8) "International Tables for X-ray Crystallography", Vol. III, Kynoch Press, Birmingham, England, p 202.
(9) C. K. Johnson, "ORTEP: A Fortran Thermal Ellipsoid Plot Program for Crystal Structure Illustrations", Oak Ridge National Laboratory, Oak Ridge, Tenn., 1965.
(10) $R = \Sigma(|F_o| - |F_c|)/\Sigma|F_o|$, $R_w = [\Sigma w(|F_o| - |F_c|)^2/\Sigma w|F_o|^2]^{1/2}$.
(11) R. M. Kirchner, T. J. Marks, J. S. Kristoff, and J. A. Ibers, *J. Am. Chem. Soc.*, **95**, 6602 (1973).
(12) G. L. Simon and L. F. Dahl, *J. Am. Chem. Soc.*, **95**, 783 (1973).
(13) R. J. Doedens, W. T. Robinson, and J. A. Ibers, *J. Am. Chem. Soc.*, **89**, 4323 (1967).
(14) L. F. Dahl and C. H. Wei, *Acta Crystallogr.*, **16**, 611 (1963).
(15) J.-C. Zimmer and H. Huber, *C. R. Acad. Sci., Ser. C*, **267**, 1685 (1968).
(16) R. D. Adams, M. D. Brice, and F. A. Cotton, *Inorg. Chem.*, **13**, 1080 (1974).
(17) J. Howard, S. A. R. Knox, F. G. A. Stone, and P. Woodward, *Chem. Commun.*, 1477 (1970).
(18) L. F. Dahl and R. E. Rundle, *Acta Crystallogr.*, **16**, 419 (1963).
(19) B. K. Teo, M. B. Hall, R. F. Fenske, and L. F. Dahl, *J. Organomet. Chem.*, **70**, 413 (1974). The labeling of the molecular orbitals used here follows that of ref 19.
(20) M. R. Churchill and S. W.-Y. Chang, *Inorg. Chem.*, **13**, 2413 (1974).
(21) B. T. Kilbourn, T. L. Blundell, and H. M. Powell, *Chem. Commun.*, 444 (1965).
(22) N. F. Gapotchenko, N. V. Alekseev, A. B. Antova, K. N. Anisimov, N. E. Kolobova, I. A. Donova, and Y. T. Struchkov, *J. Organomet. Chem.*, **23**, 525 (1970).
(23) G. M. Bancroft and K. D. Butler, *J. Chem. Soc., Dalton Trans.*, 1694 (1973).
(24) B. S. Kamrass and L. L. Lohr, private communication.
(25) D. A. Brown, W. J. Chambers, N. J. Fitzpatrick, and R. M. Rawlinson, *J. Chem. Soc. A*, 720 (1971).
(26) F. A. Cotton and J. M. Troup, *J. Am. Chem. Soc.*, **96**, 5070 (1974).